First-principles study of structure and nonlinear optical properties of $CdHg(SCN)_4$ crystal*

Zhang Peng(张 鹏)[a], Kong Chui-Gang(孔垂岗)[a], Zheng Chao(郑 超)[a], Wang Xin-Qiang(王新强)[b], Ma Yue(马 跃)[a], Feng Jin-Bo(冯金波)[a], Jiao Yu-Qiu(矫玉秋)[a], and Lu Gui-Wu(卢贵武)[a]†

[a] College of Science, China University of Petroleum, Beijing 102249, China
[b] State Key Laboratory of Crystal Materials and Institute of Crystal Materials, Shandong University, Jinan 250100, China

(Received 6 May 2014; revised manuscript received 7 July 2014; published online 10 December 2014)

The geometric structure, electronic structure, and optical properties of $CdHg(SCN)_4$ crystal are calculated by using the density functional perturbation theory and Green function screening Coulomb interaction approximation. The band gap of $CdHg(SCN)_4$ crystal is calculated to be 3.198 eV, which is in good agreement with the experimental value 3.265 eV. The calculated second-order nonlinear optical coefficients are $d_{14} = 1.2906$ pm/V and $d_{15} = 5.0928$ pm/V, which are in agreement with the experimental results ($d_{14} = (1.4 \pm 0.6)$ pm/V and $d_{15} = (6.0 \pm 0.9)$ pm/V). Moreover, it is found that the contribution to the valence band mainly comes from Cd-4d, Hg-5d states, and the contributions to the valence band top and the conduction band bottom predominantly come from C-2p, N-2p, and S-3p states. The second-order nonlinear optical effect of $CdHg(SCN)_4$ crystal results mainly from the internal electronic transition of $(SCN)^-$.

Keywords: $CdHg(SCN)_4$ crystal, nonlinear optical properties, band gap, Green function screening Coulomb interaction approximation, density functional perturbation theory

PACS: 42.70.Mp, 61.50.Ah, 71.20.–b **DOI:** 10.1088/1674-1056/24/2/024221

1. Introduction

Nonlinear optical (NLO) crystal materials are widely used in the area of optical computing, optical communications, optical data storage, switching, amplification, and signal processing. In recent decades, a number of NLO crystals with good performances have been synthesized, and their structures and optical properties have been studied. In particular, researchers in Shandong University have synthesized a series of bimetallic coordination compounds *AB*TC (*A* = Mg, Ca, Sr, Ba, Mn, Fe, Cu, Zn, Co, Ni, and Cd; *B* = Co, Zn, Cd, and Hg), and Yuan *et al*. have studied the crystal structures and the NLO properties of some compounds.[1] The results show that the second harmonic generation (SHG) efficiency of the crystal powder of $CdHg(SCN)_4$ is 13 times larger than that of urea, and $CdHg(SCN)_4$ possesses a good thermal stability and high laser damage threshold. However, the physics mechanism of NLO effect for *AB*TC crystal is not clear to our knowledge. So a further theoretical study and physical understanding of it are desired.

In theoretical study, the energy band structures are usually calculated in the local density approximation (LDA) or generalized gradient approximation (GGA) based on the density-functional theory (DFT). However, it is known that the band gaps are always underestimated if the calculation is based on the DFT and the calculated band gap generally requires correction, no matter what approximation method is used.[2,3] There are some methods of correcting the calculations, such as Green function screening Coulomb interaction (GW) approximation,[4–6] hybrid density-functional theory,[7] self-interaction–correction methods,[8] etc. Among these methods, the GW approximation is regarded as the most reliable. In this paper, the energy band structure of CMTC crystal is computed and their second-order NLO properties are studied with the GW approximation method and the density functional perturbation theory (DFPT).

2. Computational methods

2.1. Green function screening interaction approximation method

The GW approximation is based on the set of Hedin's equations that, when solved self-consistently, yield the exact interacting single-particle Green function.[9] In the GW approximation, the vertex corrections are neglected, resulting in a simplified self-energy Σ_{xc} equation, i.e.,

$$\Sigma_{xc}(\boldsymbol{r}, \boldsymbol{r}'; \omega) = \mathrm{i} \int \frac{\mathrm{d}\omega'}{2\pi} \mathrm{e}^{\mathrm{i}\omega'\delta} G(\boldsymbol{r}, \boldsymbol{r}'; \omega + \omega') W(\boldsymbol{r}, \boldsymbol{r}'; \omega'), \quad (1)$$

where δ is a positive infinitesimal number, and G and W are the electron Green function and dynamically screened

*Project supported by the National Natural Science Foundation of China (Grant No. 51372140), the Youth Scientist Fund of Shandong Province, China (Grant No. BS2011CL025), and the Basic Discipline Research Fund of China University of Petroleum, Beijing, China (Grant No. 01JB0169).

†Corresponding author. E-mail: lugw@cup.edu.cn

© 2015 Chinese Physical Society and IOP Publishing Ltd

Coulomb interaction, respectively. Hedin's equations even in the GW approximation form are still very complicated. In practice, further approximations are introduced, in which both G and W operators are constructed in the quasi-particle approximation by using the Kohn–Sham wave functions ψ_n and energies e_n obtained from the DFT calculations. Therefore, it is called the G_0W_0 or one-shot GW approximation, where G_0 is the electron Green function and is given as

$$G_0\left(\boldsymbol{r},\boldsymbol{r}';\omega\right)=\sum_n\frac{\psi_n(\boldsymbol{r})\psi_n^*(\boldsymbol{r}')}{\omega-e_n}, \tag{2}$$

and W_0 is the dynamically screened Coulomb interaction

$$W_0\left(\boldsymbol{r},\boldsymbol{r}';\omega\right)=\int \mathrm{d}r''\varepsilon^{-1}(\boldsymbol{r},\boldsymbol{r}'';\omega)V(\boldsymbol{r}'',\boldsymbol{r}'), \tag{3}$$

$$\varepsilon\left(\boldsymbol{r},\boldsymbol{r}';\omega\right)=\delta(\boldsymbol{r},\boldsymbol{r}')-\int \mathrm{d}r''P_0(\boldsymbol{r},\boldsymbol{r}'';\omega)V(\boldsymbol{r}'',\boldsymbol{r}'), \tag{4}$$

$$P_0\left(\boldsymbol{r},\boldsymbol{r}';\omega\right)=-\frac{\mathrm{i}}{2\pi}\int \mathrm{d}\omega' G_0(\boldsymbol{r},\boldsymbol{r}';\omega+\omega')G_0(\boldsymbol{r}',\boldsymbol{r};\omega'), \tag{5}$$

with V being the bare Coulomb interaction, and ε^{-1} the inverse dielectric matrix.

The energies ε_n are calculated by using the first order perturbation theory, and the perturbation is written as

$$\delta\Sigma_{\mathrm{xc}}=\Sigma_{\mathrm{xc}}-V_{\mathrm{xc}}, \tag{6}$$

where V_{xc} is the exchange correlation potential perturbation. The energies

$$\varepsilon_n=e_n+z_n(e_n)(\delta\Sigma_{\mathrm{xc}})_n(e_n), \tag{7}$$

where

$$z_n(E)=\left[1-\left(\frac{\partial}{\partial\omega}\Re\left\langle\psi_n\right|\Sigma_{\mathrm{xc}}(\omega)\left|\psi_n\right\rangle\right)_{\omega=E}\right]^{-1}. \tag{8}$$

2.2. Nonlinear optical properties

When a light beam transmits through a crystal, the crystal will be polarized by the electric field E. For a weak electric field, the relation between the dielectric polarization P and E is linear. For a strong electric field, however, the linear relation is no longer valid and we can write P as a power series of the electric field as follows:

$$P_i=P_i^s+\sum_{j=1}^{3}\chi_{ij}^{(1)}E_j+\sum_{i,j=1}^{3}\chi_{ijl}^{(2)}E_lE_j+\cdots, \tag{9}$$

where P_i^s is the zero-field polarization. In the literature dealing with nonlinear optics, one often finds another definition of the NLO susceptibility. Instead of $\chi_{ijl}^{(2)}$, it is more convenient to rely on the d tensor defined as

$$d_{ijl}=1/2\chi_{ijl}^{(2)}. \tag{10}$$

The matrix of d_{ijl} consists of 18 tensor elements. According to the symmetry of $I\bar{4}$ space group, the nonzero elements are listed as follows:[10]

$$d=\begin{pmatrix}0&0&0&d_{14}&d_{15}&0\\0&0&0&d_{24}&d_{25}&0\\d_{31}&d_{32}&0&0&0&d_{36}\end{pmatrix}. \tag{11}$$

According to Kleinman symmetry,[10] which was devised by Kleinman in 1960, $d_{24}=d_{31}=d_{32}=d_{15}$ and $d_{36}=d_{25}=d_{14}$. So, only d_{14} and d_{15} have nonzero values in the matrix element of d_{IJ}, $I=1,2,3$; $J=1,2,3,4,5,6$.

According to the DFPT,[11] we can relate the NLO susceptibilities to a third-order derivative of the energy with respect to an electric field as follows:

$$\chi_{ijl}^{(2)}=-\frac{3}{\Omega_0}F^{E_iE_jE_l}, \tag{12}$$

where Ω_0 is the unit volume and $F^{E_i}F^{E_j}F^{E_l}$ is defined as

$$\begin{aligned}F^{E_iE_jE_l}=&\frac{1}{6}(\tilde{F}^{E_iE_jE_l}+\tilde{F}^{E_iE_lE_j}+\tilde{F}^{E_jE_iE_l}\\&+\tilde{F}^{E_jE_lE_i}+\tilde{F}^{E_lE_iE_j}+\tilde{F}^{E_lE_jE_i}),\end{aligned} \tag{13}$$

and

$$\begin{aligned}\tilde{F}^{E_iE_jE_l}=&\frac{-e}{M_k}\Re\sum_{\boldsymbol{K}}\sum_{\boldsymbol{b}}w_{\boldsymbol{b}}(\boldsymbol{b}\cdot G)\\&\times\left[2\sum_{n,m}\left\langle u_{n\boldsymbol{K}}^{E_i}\middle|u_{m\boldsymbol{K}+\boldsymbol{b}}^{E_l}\right\rangle Q_{mn}(\boldsymbol{K},\boldsymbol{K}+\boldsymbol{b})\right.\\&-\sum_{n,m,n',m'}S_{mn}^{E_i}(\boldsymbol{K},\boldsymbol{K}+\boldsymbol{b})Q_{nn'}(\boldsymbol{K},\boldsymbol{K}+\boldsymbol{b})\\&\left.\times S_{n'm'}^{E_l}(\boldsymbol{K},\boldsymbol{K}+\boldsymbol{b})Q_{m'm}(\boldsymbol{K},\boldsymbol{K}+\boldsymbol{b})\right]\\&+\frac{2}{M_k}\sum_{\boldsymbol{K}}\sum_{n,m}[\delta_{m,n}\langle u_{n\boldsymbol{K}}^{E_i}|v_{\mathrm{hxc}}^{E_j}|u_{m\boldsymbol{K}}^{E_l}\rangle\\&-\langle u_{m\boldsymbol{K}}^{(0)}|v_{\mathrm{hxc}}^{E_j}|u_{n\boldsymbol{K}}^{(0)}\rangle\langle u_{n\boldsymbol{K}}^{E_i}|u_{m\boldsymbol{K}}^{E_j}\rangle]\\&+\frac{1}{6}\int\mathrm{d}\boldsymbol{r}\,\mathrm{d}\boldsymbol{r}'\,\mathrm{d}\boldsymbol{r}''\frac{\delta^3E_{\mathrm{xc}}[n^0]}{\delta n(\boldsymbol{r})\delta n(\boldsymbol{r}')\delta n(\boldsymbol{r}'')}\\&\times n^{E_i}(\boldsymbol{r})n^{E_j}(\boldsymbol{r}')n^{E_l}(\boldsymbol{r}''),\end{aligned} \tag{14}$$

where M_k is the number of k-points, $M_k=4\times4\times4=64$, E_{xc} is the exchange–correlation energy function, $n(r)$ is the ground-state density, v_{hxc} is the exchange–correlation potential which is a function of the ground-state density $n(\boldsymbol{r})$, $\boldsymbol{b}$ is the vector connecting a k-point to one of its nearest neighbours, $w_{\boldsymbol{b}}$ is a weight factor, $\boldsymbol{G}$ is a basis vector of the reciprocal lattice, S is the overlap matrix between Bloch functions at $\boldsymbol{K}$ and $\boldsymbol{K}+\boldsymbol{b}$, Q is the inverse of the overlap matrix S, and u is the projection of the first-order wave function on the conduction band.

The total energy, electronic structure, band gap, and second-order NLO susceptibilities are calculated using the ABINIT software package.[12] During the calculation, norm-conserving pseudopotential[13] was used, the cut-off energy is

22 Hatree (1 Hatree = 27.2114 eV), and the k-point grid is $4\times4\times8$ Monkhorst–Pack[14] in the irreducible Brillouin zone. At first, the structure of CMTC crystal is optimized. The structure is relaxed until the tolerance for absolute difference of total energy below 1.0×10^{-9} Hartree (1 Hartree = 27.2114 eV) is reached. The band number is set to be 400 to guarantee the converge.

3. Results and discussion

3.1. Geometric structure

The space structure of the CMTC crystal is shown in Fig. 1. The CMTC crystal belongs to a tetragonal crystallographic system, $I\bar{4}$ a space group. The lattice constants and bond lengths of CMTC crystal are listed in Table 1. One can see from Table 1 that the calculated lattice constants and bond lengths are in agreement with the experimental data.

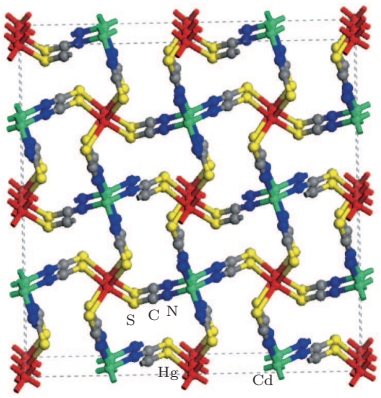


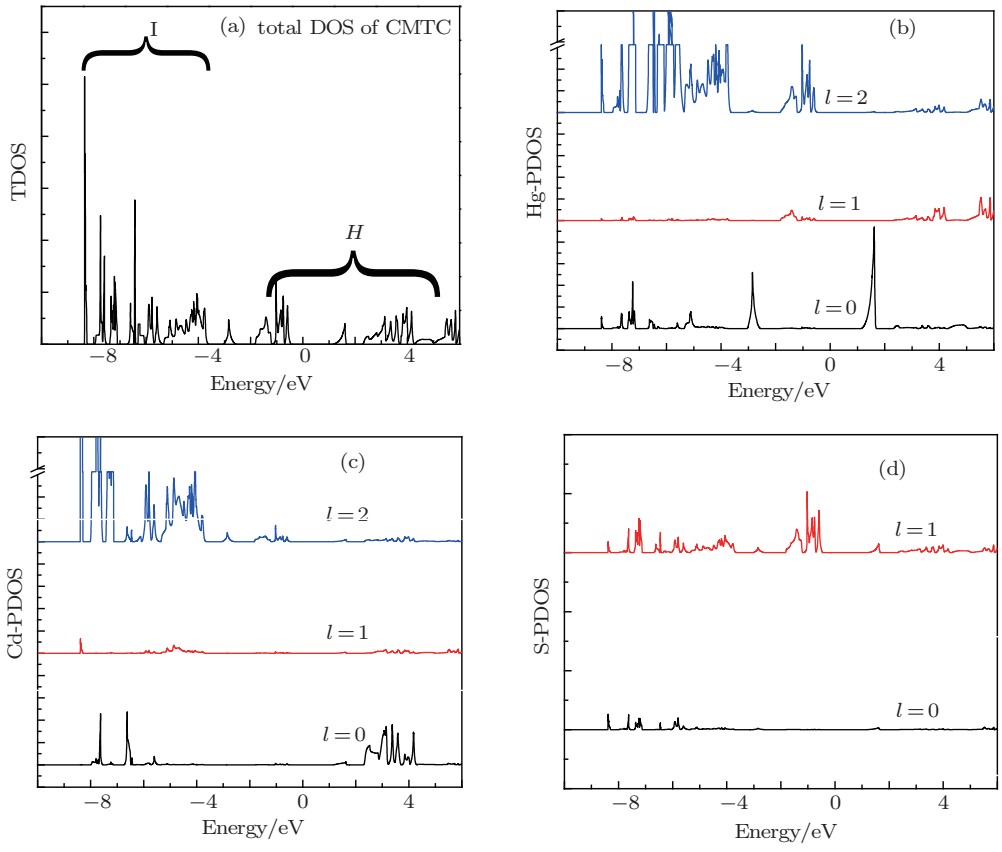
Fig. 1. (color online) Space structure of CMTC crystal.

Table 1. Lattice constants and bond lengths of CMTC crystals.

Lattice constant/nm	Calculated value	Experimental value[1]
a	1.148	1.149(2)
c	0.433	0.425(2)
Bond lengths/nm	Calculated value	Experimental value[15]
S–C	0.164	0.1655(8)
C–N	0.111	0.1148(11)
Cd–N	0.220	0.2174(8)
S–Hg	0.259	0.2574(2)

3.2. Electronic structure

In order to obtain an insight into the contributions to the band structure from Cd, Hg, S, C, and N, the total density of states (TDOS) and partial density of states (PDOS) are computed using a smearing technique and obtained from the eigenvalues, properly weighted at each k point. The calculated TDOS spectrum of the CMTC crystal is shown in Fig. 2(a). The PDOS is computed by using the tetrahedron method. We show the PDOS spectra as well as the angular-momentum projected ($l = 0, 1, 2$) DOS in Figs. 2(b)–2(f) in which the orbitals $l = 0, 1, 2$ represent s, p, and d orbitals, respectively.



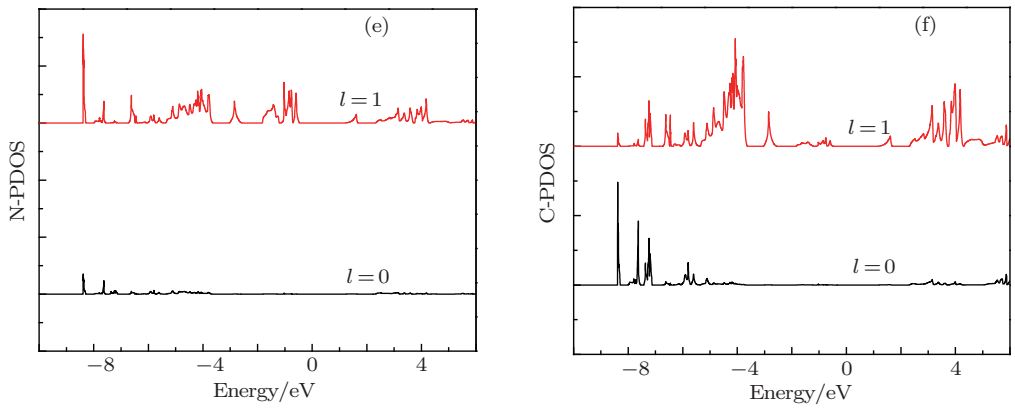


Fig. 2. (color online) (a) TDOS, (b) Hg-PDOS, (c) Cd-PDOS, (d) S-PDOS, (e) N-PDOS, (f) C-PDOS of CMTC crystals.

The TDOS spectral lines are divided into H and I groups, as shown in Fig. 2(a). By comparing them with PDOS spectral lines of CMTC crystal (Figs. 2(b)–2(f)), it can be concluded that the peak *I* (from −8.57 eV to −0.41 eV) is for the valence band which is formed mainly from Cd-4d, Hg-5d states, and the valence band top predominantly comes from C-2p, N-2p, and S-3p states. The *H* group (2.04 eV to 6 eV) is for the conduction band, which is dominantly formed by the C-2p and N-2p states.

The structure of electronic bands for the CMTC crystal in the vicinity of the forbidden gap is shown in Fig. 3. As can be seen from the figure, the energy band trend is gentler and the bandwidth is small, which is consistent with the complex compound structure of the CMTC crystal. It can be seen that the bottom of conduction band and the top of valence band are both at the same point *G* in the Brillouin zone. Thus, the CMTC crystal is a direct band gap crystal. The calculated energy gap of CMTC is 3.198 eV, which is close to the experimental value of 3.265 eV.[16]

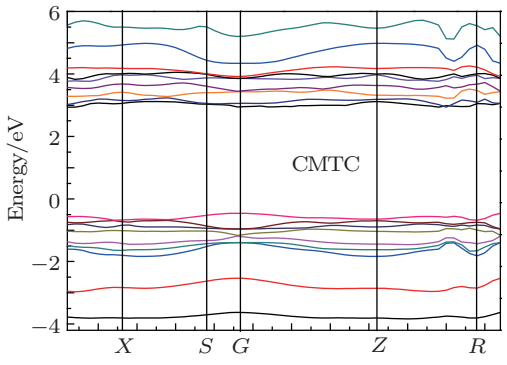


Fig. 3. (color online) Energy band of CMTC crystal.

3.3. Nonlinear optical properties

Second-order NLO susceptibilities (i.e., SHGs) are studied by using DFPT, and the parameters used are kept the same as the calculations in the GW approximation. Table 2 presents the SHG of CMTC crystal. One can notice from Table 2 that the SHGs of the CMTC crystal are in agreement with the experimental values.

Table 2. Second-order nonlinear optical susceptibilities of a CMTC crystal.

Second-order NLO coefficient	Calculated value	Experimental [17] value
d_{14}/(pm/V)	1.2906	1.4 ± 0.6
d_{15}/(pm/V)	5.0928	6.0 ± 0.9

The second-order NLO effect of crystal is mainly due to the electronic transition between the valence band top and the conduction band bottom,[18] which indicates that the electron transition in CMTC crystal is the dominant mechanism for SHG. In order to investigate the NLO effect in detail, in this paper the SHG dependence on energy band of CMTC crystal is studied using the energy band structure decomposition method. It is found that occupied states above −1 eV have a significant effect on the SHG of a CMTC crystal, while the unoccupied states between 3 eV and 6 eV are the main sources for NLO properties. Compared with PDOSs shown in Fig. 2, these occupied states come mainly from N-2p and S-3p orbitals, and the unoccupied states originate mainly from C-2p and N-2p orbitals. Therefore, we can conclude that the SHG effect of CMTC results from the electron transition between the valence band (containing N-2p and S-3p orbitals) and the empty band (containing C-2p and N-2p orbitals).

4. Conclusions

The structural, electronic, linear, and nonlinear optical properties of a CMTC crystal are studied by the quantum-mechanical calculations based on the GW approximation method and DFPT, and the computed results are in good agreement with the experimental values. Our analysis of the band structure shows that the contributions to the valence band bottom mainly come from Cd-4d, Hg-5d. Moreover, the contributions to the valence band top and the conduction band bottom

predominantly come from C-2p, N-2p, and S-3p states. The second-order NLO effects of a CMTC crystal are mainly due to the internal electronic transition in $(SCN)^-$. These conclusions are consistent with the results from the anionic group theory suggested by Cheng Chuang-Tian.[18] The calculated results show that CMTC has good second-order NLO susceptibilities and can be used as a kind of promising crystal material in the NLO field.

References

[1] Yuan D R, Xu D, Liu M G, Yu W T, Fang Q, Hou W B, Bing Y H, Sun S Y and Jiang M H 1996 *Chin. Sci. Bull.* **41** 1572

[2] Chen D, Xiao H Y, Jia W, Chen H, Zhou H G, Li Y, Ding K N and Zhang Y F 2012 *Acta Phys. Sin.* **61** 127103 (in Chinese)

[3] Yu B H and Chen D 2014 *Acta Phys. Sin.* **63** 047101 (in Chinese)

[4] Usuda M, Hamada N, Kotani T and Schilfgaarde M 2002 *Phys. Rev. B* **66** 125101

[5] Zhu X J and Louie S G 1991 *Phys. Rev. B* **43** 14142

[6] Lu T Y and Huang M C 2007 *Chin. Phys.* **16** 62

[7] Patterson C H 2006 *Phys. Rev. B* **74** 144432

[8] Perdew J P and Zunger A 1981 *Phys. Rev. B* **23** 5048

[9] Jiang H 2010 *Acta Phys. Chim. Sin.* **26** 1017

[10] Qian S X and Wang G M 2001 *Nonlinear Optics* (Shanghai: Fudan University Press) pp. 28–31, 67–69, 577–578 (in Chinese)

[11] Marek V 2005 "First-principles Study of the Nonlinear Responses of Insulators to Electric Fields: Applications to Ferroelectric Oxides" (Ph. D. Dissertation) (De Liege: Faculté des Sciences of University De Liege)

[12] Gonze X, Rignanese G M, Verstraete M, Beuken J M, Pouillon Y, Caracas R, Jollet F, Torrent M, Zerah G, Mikami M, Ghosez P, Veithen M, Raty J Y, Olevano V, Bruneval F, Reining L, Godby R, Onida G, Hamann D R and Allan D C 2005 *Z. Kristallogr* **220** 558

[13] Hamann D R, Schlüter M and Chiang C 1979 *Phys. Rev. Lett.* **43** 1494

[14] Monkhorst H J and Pack J D 1976 *Phys. Rev. B* **13** 5188

[15] Yan Y X, Feng Q, Yuan D R, Tian Y P, Liu Z, Wang X M, Jiang M H, Williams D, Siu A and Cai Z G 1999 *Chin. Chem. Lett.* **10** 257

[16] Yuan D R, Xu D, Liu M G, Qi F, Yu W T, Hou W B, BingY H, Sun S Y, Liu M H and Liu J 1997 *Appl. Phys. Lett.* **70** 544

[17] Zhang G H, Liu M G, Xu D and Yuan D R 2000 *J. Mater. Sci. Lett.* **19** 1255

[18] Lin Z S, Wang Z Z, Chen C T and Li M X 2001 *Acta Phys. Sin.* **50** 1145 (in Chinese)